



Tema: Engenharia de superfície

## MICRO-ABRASIVE WEAR RESISTANCE OF LOW-TEMPERATURE PLASMA CARBURIZED MARTENSITIC STAINLESS STEEL \*

Cristiano José Scheuer<sup>1</sup>  
Júlio Cesar Klein das Neves<sup>2</sup>  
Rodrigo Perito Cardoso<sup>3</sup>  
Sílvio Francisco Brunatto<sup>3</sup>

### Abstract

The effect of low-temperature plasma carburizing treatment on the micro-abrasive wear resistance of AISI 420 steel was investigated by mean of a CSM Calowear ball-cratering equipment. Carburized samples were treated at temperatures of 350, 400, 450 and 500°C for a fixed time of 12 h, using a gas mixture containing 99.5% (80% H<sub>2</sub>+20% Ar)+0.5% CH<sub>4</sub>. Micro-scale abrasive wear tests were conducted with a 25.4 mm AISI 420 steel sphere, using an abrasive suspension of alumina (Al<sub>2</sub>O<sub>3</sub>) with particle size of 1 µm (abrasive concentration of 0.11 g/cm<sup>3</sup>). The contact normal force, abrasive flow and ball rotation speed were fixed at: 0.5 N, 0,2 drop/s, and 120 rpm. The wear craters were analyzed using a confocal laser microscope, Olympus OLS 3000. The wear analyses were performed for test times of: 30, 60, 90, 120, 180, 360, 540, 720 and 900 s (equivalent sliding distance: 0.84, 1.68, 2.52, 3.36, 5.04, 10.09, 15.14, 20.19 and 25.23 m, respectively). The results indicate that the wear coefficient in the outer layer and in the diffusion layer are different, being lower in the latter. It was also verified that the wear coefficient on the outer layer region decreases with increasing treatment temperature in the range of 350 to 450 °C, and increase again for 500°C. The diffusion layer wear coefficient is similar for all the carburized samples. Finally, for all studied conditions, the analysis of the wear craters surface indicates the occurrence of grooving and micro-rolling abrasion wear modes.

**Keywords:** Ball-cratering test; Micro-abrasive wear resistance; Grooving abrasion wear; Micro-rolling abrasion wear; Plasma carburizing; Martensitic stainless steel.

<sup>1</sup> Plasma Assisted Manufacturing Technology & Powder Metallurgy Group, Departamento de Engenharia Mecânica, UFPR, Colégio Técnico Industrial de Santa Maria, UFSM, Curitiba, PR, Brazil.

<sup>2</sup> Departamento Acadêmico de Mecânica, UTFPR, Curitiba, PR, Brazil.

<sup>3</sup> Colégio Técnico Industrial de Santa Maria, UFSM, Santa Maria, RS, Brazil.

\* Technical contribution to the 1<sup>st</sup> Workshop on surface treatments of corrosion resistant alloys, July 21<sup>st</sup> -25<sup>th</sup>, 2014, São Paulo, SP, Brazil.



## 1 INTRODUCTION

Martensitic stainless steels (MSS) are usually employed as engineering materials due to its interesting combination of mechanical properties and corrosion resistance [1]. However, in some tribological applications, it is necessary to improve the material surface properties keeping the bulk properties unchanged. Therefore, there is an increasing interest in improving surface properties of MSS and plasma assisted thermochemical treatments can be applied for this purpose [2]. Thereby several studies were carried out investigating the effect of plasma nitriding treatment on the wear behaviour of the MSS [2-6]. Otherwise, the influence of plasma carburizing on MSS wear properties has been only studied and reported by Li and Bell [7], presenting non promising results. A new perspective on plasma carburizing of MSS has presented by Scheuer *et al.* [8-10], where it was established that an adequate choice of carburizing treatment parameters can lead to important improvements of the MSS treated surface mechanical properties. Based on this new perspective, the aim of the present work is to study the effect of low-temperature plasma carburizing on the micro-abrasive wear resistance of AISI 420 martensitic stainless steel.

## 2 EXPERIMENTAL PROCEDURE

Cylindrical samples of 10 mm in height and 50.8 mm in diameter were cut from an AISI 420 steel commercial rod (composition obtained by X-ray fluorescence, in wt.%: 0.17% C, 0.70% Mn, 0.50% Si, 12.2% Cr, 0.23% P, 0.03% S, and Fe balance). Samples were air quenched from 1050°C, after 1 h at the austenitizing temperature. The sample hardness in the as-quenched condition was  $510 \pm 10$  HV<sub>0.3</sub>. After heat treatment, samples were ground using SiC sandpaper ranging from 100 to 1200 grade and polished using 1 µm Al<sub>2</sub>O<sub>3</sub> abrasive suspension. Finally, samples were alcohol cleaned in ultrasonic bath and then introduced into the discharge chamber.

A schematic representation and the description of the plasma carburizing apparatus used in the present work is shown in ref. [10]. In this system, samples were placed on the cathode of the discharge, which was negatively biased at 700 V. Aiming to remove the native oxide layer from sample surface, before carburizing, specimens were plasma sputter-cleaned in a gas mixture of 80% H<sub>2</sub> + 20% Ar, under a pressure of 400 Pa, at 300°C for 0.5 h. Plasma carburizing was carried out using a gas mixture composed of 99.5% (80% H<sub>2</sub> + 20% Ar) + 0.5% CH<sub>4</sub>, in volume. The total gas flow rate and pressure were fixed at  $1.66 \times 10^{-6}$  Nm<sup>3</sup> s<sup>-1</sup> (100 sccm) and 400 Pa, respectively. The gas mixture composition and flow rate were fixed according to [9], pressure and applied voltage according to [11] and [12], respectively. Samples were carburized at 350, 400, 450 and 500 °C, for a constant treatment time of 12 h.

Micro-abrasive wear tests were performed using a CSM CaloWear<sup>®</sup> microabrasion ball-cratering equipment (Figure 1). For this work, a AISI 420 steel ball, with diameter of 25.4 mm and an abrasive suspension of Al<sub>2</sub>O<sub>3</sub> particles, with an average particle size of 1 µm, and concentration of 0.11 g/cm<sup>3</sup> was applied. The abrasive suspension was continuously agitated during the wear test by means of stirring apparatus attached to the microabrasion equipment, in order to prevent the decantation of abrasive particles. The suspension was pumped to the ball/sample interface by a peristaltic pump, being the flow rate fixed at 1 drop/5 s. The drive shaft rotation speed was kept constant at 120 rpm, generating a velocity between the sphere and the sample surface of approximately 0.2 m s<sup>-1</sup>. The diameter of the produced craters

\* Technical contribution to the 1<sup>st</sup> Workshop on surface treatments of corrosion resistant alloys, July 21<sup>st</sup> -25<sup>th</sup>, 2014, São Paulo, SP, Brazil.



were measured after wear test times of 30, 60, 90, 120, 180, 360, 540, 720 and 900 s totaling a sliding distance of 0.84, 1.68, 2.52, 3.36, 5.04, 10.09, 15.14, 20.19 and 25.23 m, respectively. From measuring of the worn craters diameter, the wear volume was determined for each test applying the equations suggested by [13] (the presented value of wear volume is the average of three test for each testing conditions). The wear coefficient was determined from the line slope generated by the data linearization of the function  $V = f(L, F_N)$ , where,  $V$  is the wear volume;  $L$  is the sliding distance; and  $F_N$  the normal contact force. The normal contact force employed in this work was  $0.5 \pm 0.05$  N. The worn region (wear crater) was analyzed by confocal laser scanning microscope (Olympus LEXT OLS 3000), aiming to identify the abrasion wear mode.

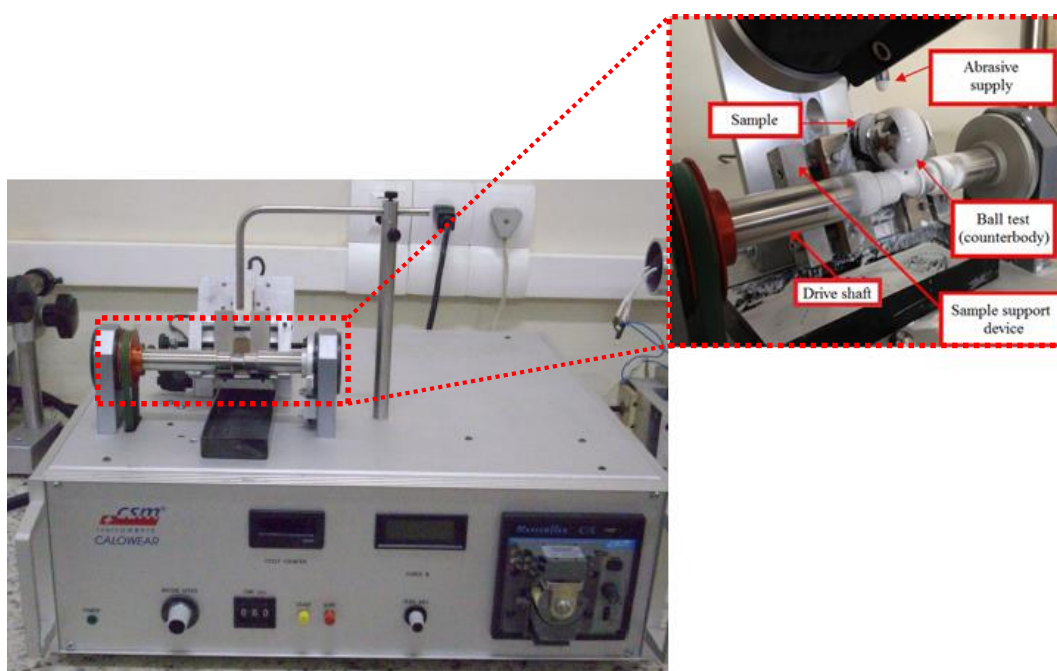


Figure 1. Experimental setup of CaloWear ball-cratering equipment applied for microabrasion test.

### 3 RESULTS AND DISCUSSION

#### 3.1 Wear Coefficient

The abrasive wear coefficients were calculated using the linearization of the wear volume data as a function of sliding distance times normal force ( $V = f(L, F_N)$ ) – Figure 2, considering that the  $V$  varies with  $L \cdot F_N$  following the Archard equation [13]. According to Archard equation, the slope of the line generated by data points shown in Figure 2 determines an average value of the wear coefficient. Looking at Figure 2, it appears that for the carburized samples two slopes can be observed for the  $V = f(L, F_N)$  data, indicating the occurrence of different wear coefficients in the same sample. In this case, this result is possibly a consequence of the carburized layer configuration (outer layer + diffusion layer) presenting different characteristics/properties along its section. As discussed in [8-12], the outer layer is composed by  $\alpha'c$  (carbon expanded martensite) and  $Fe_3C$ , presenting probably higher hardness and lower toughness. On the other hand, the diffusion layer is composed of  $\alpha'c$ , presenting lower hardness and higher toughness (as compared to the outer layer). Thus, one line (greater slope) would correspond to the outer layer

\* Technical contribution to the 1<sup>st</sup> Workshop on surface treatments of corrosion resistant alloys, July 21<sup>st</sup> -25<sup>th</sup>, 2014, São Paulo, SP, Brazil.



wear coefficient and the other (lower slope) to the diffusion layer. To support this argument, on Figure 3 the variation of the worn crater depth according the sliding distance is presented. It can be noticed from Figure 3 that the first four points (related to the greatest slope line in Figure 2) reveal worn crater depths of about 3  $\mu\text{m}$ , being this depth equivalent to the outer layer thickness. Above this value material removal from the diffusion layer region starts to occur. Ramalho [14], also noted the occurrence of a “nonlinear” compartment of the  $V = f(L, F_N)$  product. In this case, the author studied the micro-abrasive wear resistance of AISI M2 steel coated with a copper film of 9  $\mu\text{m}$  thickness, however, the author has not justified this wear coefficient behavior. Furthermore, it can be also verified by the analysis of Figure 2, that the untreated sample showed a linear behavior for the  $V = f(L, F_N)$  relation, result was already expected since the untreated material exhibits constant properties throughout its section. The non-linearity of the first point in relation to the others for untreated sample (Figure 2), is probably related to the non-steady state wear.

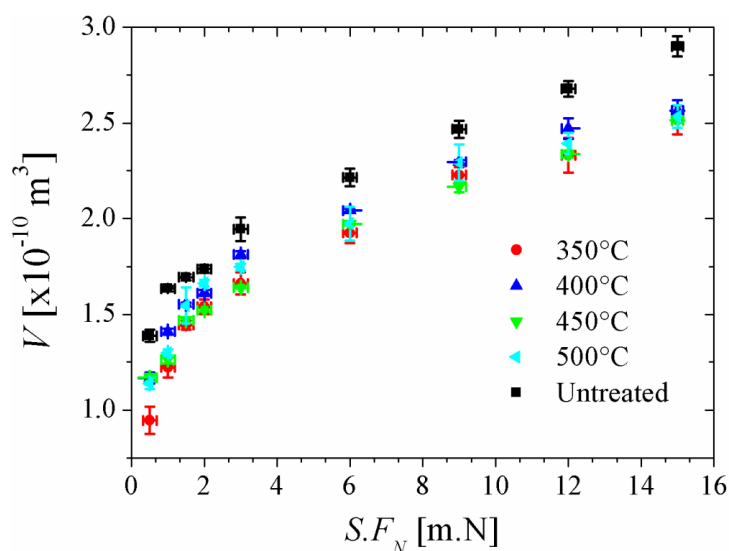


Figure 2. Plot of the wear volume as a function of the product of sliding distance and normal load. Tests performed employing a normal force of 0.5 N, ball rotational speed of 120 rpm and 1- $\mu\text{m}$  alumina abrasive flow rate of 1 drop/5 s.

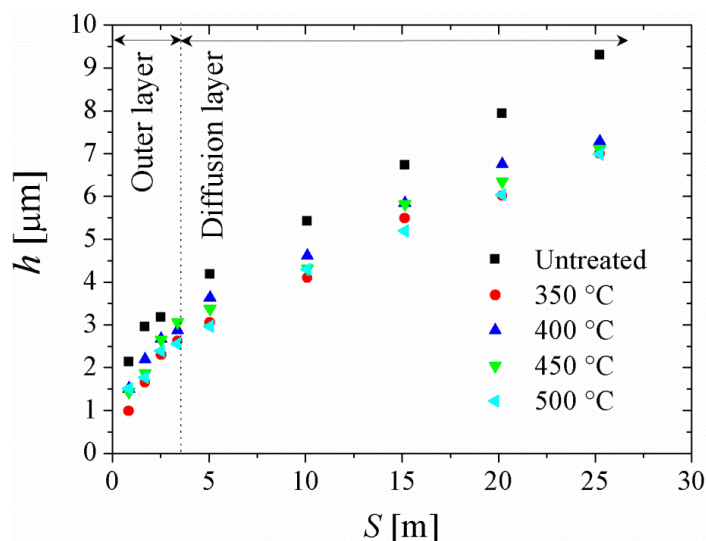


Figure 1 Wear crater depth as a function of sliding distance. Tests performed employing a normal force of 0.5 N, ball rotational speed of 120 rpm and 1- $\mu\text{m}$  alumina abrasive flow rate of 1 drop/5 s.

\* Technical contribution to the 1<sup>st</sup> Workshop on surface treatments of corrosion resistant alloys, July 21<sup>st</sup> -25<sup>th</sup>, 2014, São Paulo, SP, Brazil.



The wear coefficient as a function of carburizing temperature and the value for the untreated sample is presented on Figure 4. It can be observed that the outer layer wear coefficient presents for all studied carburizing conditions, a considerably higher value than the untreated sample. The reason may be related to the high hardness of the outer layer (563.4, 646.0, 850.4 and 987.5 HV<sub>0.3</sub> for samples treated at 350, 400, 450 and 500 °C, respectively – untreated 510 HV<sub>0.3</sub>). According Zum Gahr [15] the abrasive wear resistance of steels diminishes with increasing hardness. This phenomenon is related to the transition of microploughing to microcutting and microcracking wear mechanisms [15]. It also appears that the outer layer wear coefficient decreases with treatment temperature increasing in the range of 350–450°C, and increase with increasing temperature from 450 to 500°C. The  $k$  variation as a function of the carburizing temperature occurs due to the nature of the metallurgical phases formed. To the interval between 350 to 450°C, the increase in the amount of Fe<sub>3</sub>C phases may be responsible for the decrease in the wear coefficient. Moreover, for the treatment condition of 500°C, the wear coefficient increase can be credited to the formation of Cr<sub>7</sub>C<sub>3</sub> and Cr<sub>23</sub>C<sub>6</sub> phases (details can be found in Scheuer *et al.* [10]). Moreover, from Figure 4 it can be seen that the diffusion layer has wear coefficient slightly lower than the untreated sample. Furthermore, the wear coefficient reduction on the diffusion layer may be related to its higher toughness. In this case, the abrasive particles primarily promote the plastic deformation of the material and then promote their pullout.

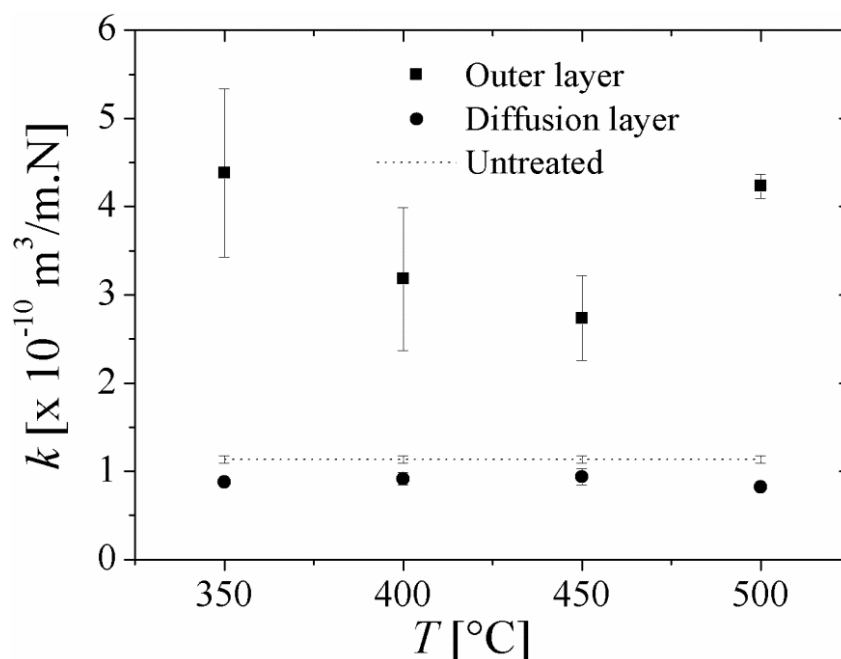


Figure 4. Wear coefficient of untreated and plasma carburized samples. Tests performed employing a normal force of 0.5 N, ball rotational speed of 120 rpm and 1- $\mu$ m alumina abrasive flow rate of 1 drop/5 s.

### 3.2 Wear Mechanism

In Figure 5 (a) and (b) a three-dimensional illustration of a typical worn crater produced by micro scale abrasive wear test is presented. This wear crater is generated by the sliding ball on the test material with a layer of abrasive slurry interposed in between. It is noted that the wear scar geometry on the test material

\* Technical contribution to the 1<sup>st</sup> Workshop on surface treatments of corrosion resistant alloys, July 21<sup>st</sup> -25<sup>th</sup>, 2014, São Paulo, SP, Brazil.



reproduces the geometric shape of the test ball. Analyzing the Figure 5 (c) it can be noted that for this magnification (200 $\times$ ) only grooving abrasion is visible. This pattern is repeated for all other carburized samples and for all tested conditions. The blackened halo observed around the crater worn in Figure 5 corresponds to corrosion, occurred during wear test due to the high PH of the abrasive suspension. The occurrence of corrosion on the worn crater was only observed in the sample carburized at 500°C. This is justified by the fact that for this treatment temperature, an intense precipitation of chromium carbides occurs at the outer layer, promoting a significant reduction in the material corrosion resistance. Chromium carbides precipitation is confirmed by micrographs and XRD data not shown here.

Figure 6 show images of the same wear crater shown in Figure 5 (c), at different magnifications (1000 $\times$  Fig. (a), 2100 $\times$  Fig. (b), and 4000 $\times$  Fig. (c)). Figure 6 (a-c) exhibit the occurrence of rolling abrasion along the grooves for a sliding distance of 6.0 m. This phenomenon (the occurrence of rolling abrasion at the surface or in between the grooves) was previously reported by Cozza [16-19], being called as micro-rolling abrasion. According Cozza *et al.* [16], the shaft misalignment was considered as a possible cause of the micro-rolling abrasion occurrence.

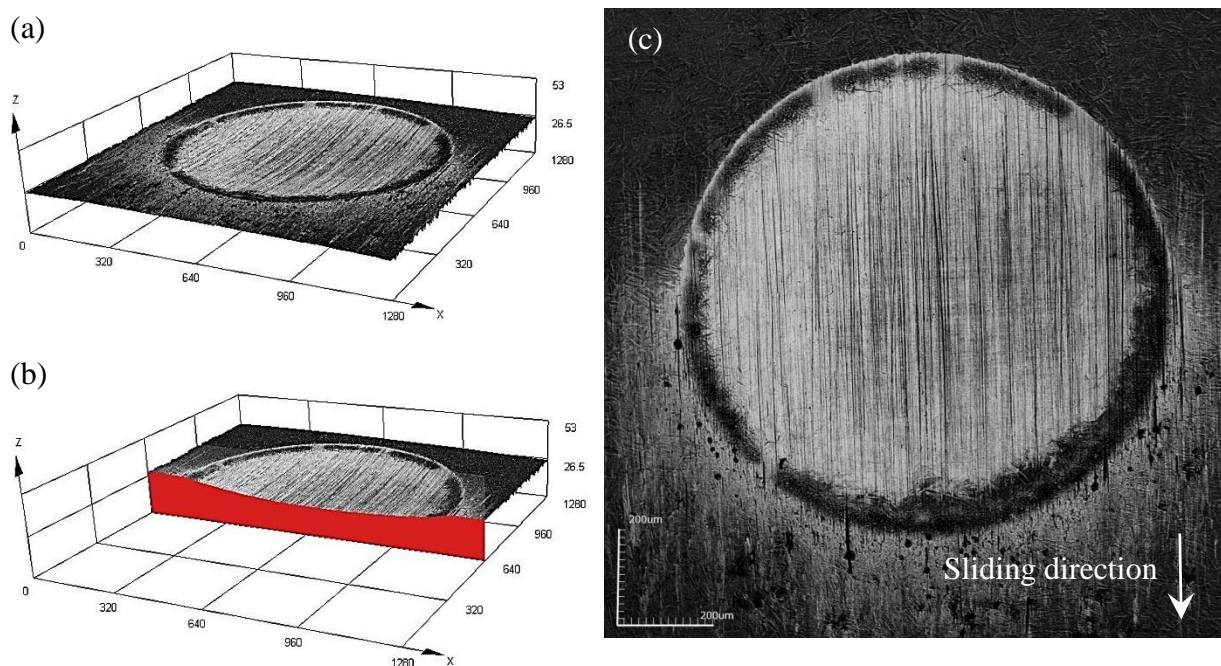


Figure 5. (a) and (b) Typical worn crater produced by micro scale abrasive wear test (3D confocal microscopy images), and (c) Wear crater front view (image magnification of 200  $\times$ ). Sample plasma carburized at 500 °C for 12 h. Wear tests performed employing a normal force of 0.5 N, ball rotational speed of 120 rpm, 1- $\mu$ m alumina abrasive flow rate of 1 drop/5 s and sliding distance of 6.0 m.

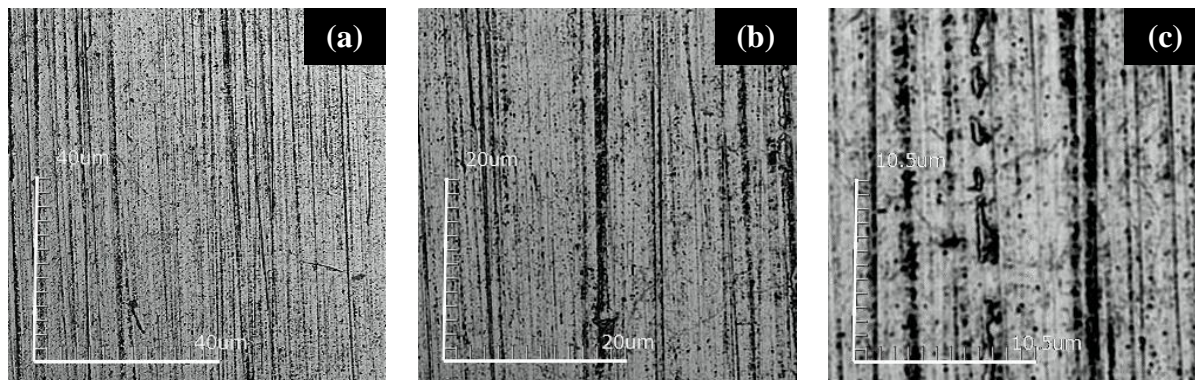


Figure 6. Wear crater front view with an image magnification of 1000x (a), 2100x (b) and 4000x (c). Sample plasma carburized at 500 °C for 12 h. Wear tests performed employing a normal force of 0.5 N, ball rotational speed of 120 rpm, 1- $\mu$ m alumina abrasive flow rate of 1 drop/5 s and sliding distance of 6.0 m.

Figure 7 (a-c) and Figure 8 (a-c) depict the presence of micro-rolling abrasion in wear craters for the sliding distance of 12.0 m and 15.0 m. A comparison between Figure 6, Figure 7 and Figure 8 suggests that the degree of micro-rolling abrasion is relatively lower in the beginning of the tests (Figure 6) and increases towards larger distances (Figure 7 and Figure 8). Cozza *et al.* [16] showed similar behavior, the authors claim that this behavior is consistent with the observed in cases where grooving abrasion and rolling abrasion are simultaneously observed (when viewed larger scale, as illustrated in Figure 3 (c) of the paper [16]). According Cozza [20] the increase in the rolling abrasion worn area with the sliding distance may be explained by considering that in the test beginning (shorter sliding distances) the contact pressure is high than at final test conditions (long sliding distances), and in that condition it is more difficult for the abrasive particles to roll to the ball/sample contact region. Looking at Figure 7 (b-c) it can be seen the formation of micro-cracks in the worn crater. Fracture due to micro-cracks is commonly seen in brittle materials that have low fracture toughness. According Sevim and Kulekci (21), micro-cracks fracture is commonly seen in brittle materials that have low fracture toughness. From the standpoint of plasma assisted treatment, among the studied conditions, the 500 °C is that showed the highest hardening. The occurrence of micro-cracks may be related to high hardness, however its occurrence only for the sliding distance of 12.0 m still remains unexplained requiring an additional study.

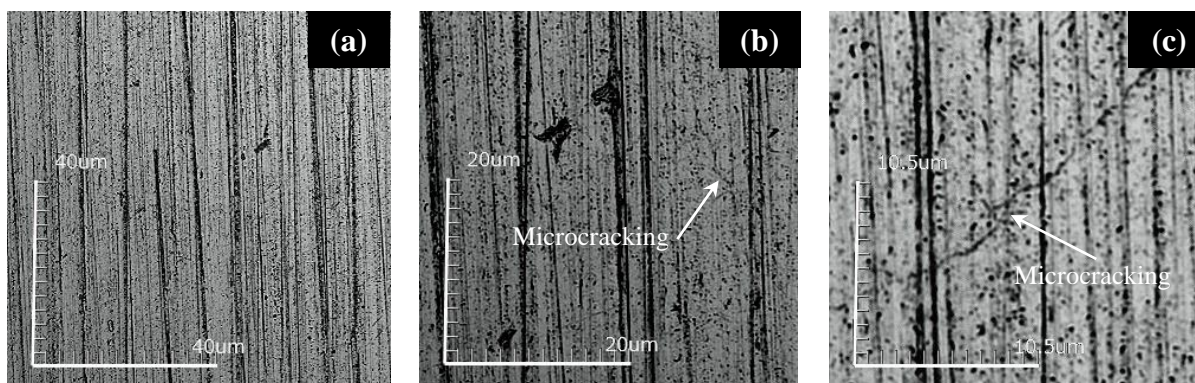


Figure 7. Wear crater front view with an image magnification of 1000x (a), 2100x (b) and 4000x (c). Sample plasma carburized at 500 °C for 12 h. Wear tests performed employing a normal force of 0.5 N, ball rotational speed of 120 rpm, 1- $\mu$ m alumina abrasive flow rate of 1 drop/5 s and sliding distance of 12.0 m.

\* Technical contribution to the 1<sup>st</sup> Workshop on surface treatments of corrosion resistant alloys, July 21<sup>st</sup> -25<sup>th</sup>, 2014, São Paulo, SP, Brazil.

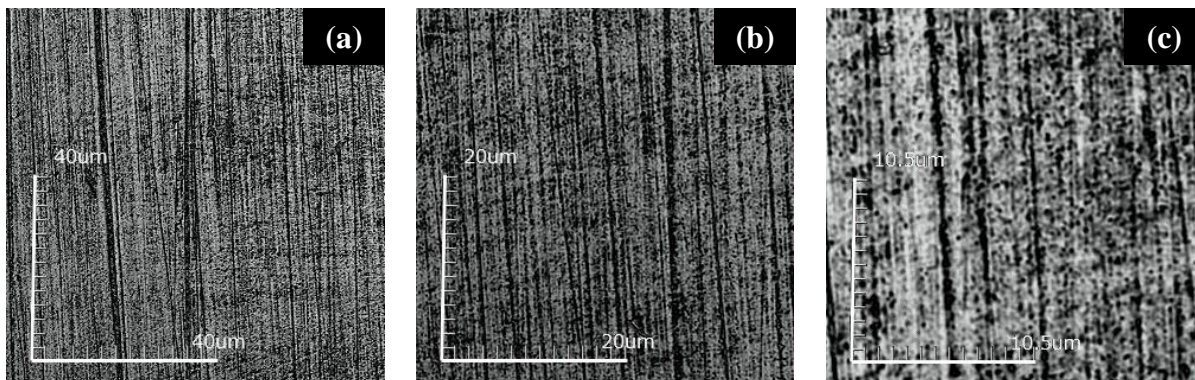


Figure 2. Wear crater front view with an image magnification of 1000x (a), 2100x (b) and 4000x (c). Sample plasma carburized at 500 °C for 12 h. Wear tests performed employing a normal force of 0.5 N, ball rotational speed of 120 rpm, 1- $\mu$ m alumina abrasive flow rate of 1 drop/5 s and sliding distance of 15.0 m.

## 4 CONCLUSION

The results obtained in this work have indicated the following:

- (a) The outer layer and diffusion layer region presents different wear coefficient. The outer layer wear coefficient is greater than the untreated sample. The diffusion layer wear coefficient is slightly lower than the untreated samples;
- (b) On the outer layer the wear coefficient decreases with the increase of the treatment temperature in the range of 350 to 450 °C and increases from 450 to 500 °C; and, on the diffusion layer, the wear coefficient shows a similar value for the studied treatment conditions;
- (c) Results demonstrated the occurrence of severe wear regime for all tested conditions;
- (d) Microscopic characterization of the worn craters indicate the occurrence of grooving and micro-rolling abrasion wear modes; It was found that the degree of micro-rolling abrasion is relatively lower in the beginning of the tests and increases towards larger distances; and,

## Acknowledgements

This work was supported by CNPq, CAPES-COFECUB and *Programa Interdisciplinar de Petróleo e Gás Natural da UFPR* (PRH24). The authors also wish to express their thanks to the Laboratory of X-ray Optics and Instrumentation (LORXI) and Surface Engineering Laboratory, from the Universidade Federal do Paraná (UFPR) by the use of the X-ray diffraction equipment and the confocal laser microscope, respectively.

## REFERENCES

- 1 Dodds SAH, Cater S. Tribological enhancement of AISI 420 martensitic stainless steel through friction-stir processing. *Wear*. 2013;302(1-2):863-877.
- 2 Corengia P, Walther F, Ybarra G, Sommadossi R, Corbari R, Broitman E. Friction and rolling-sliding wear of DC-pulsed plasma nitride AISI 410 martensitic stainless steel. *Wear*. 2006;260:479-485.
- 3 Xi Y, Liu D, Han D. Improvement of corrosion and wear resistances of AISI 420 martensitic stainless steel using plasma nitriding at low temperature. *Surface & Coatings Technology*. 2008;202:2577-2583.

\* *Technical contribution to the 1<sup>st</sup> Workshop on surface treatments of corrosion resistant alloys, July 21<sup>st</sup> -25<sup>th</sup>, 2014, São Paulo, SP, Brazil.*



- 4 Xi Y, Liu D, Han D. Improvement of mechanical properties of martensitic stainless steel by plasma nitriding at low temperature. *Acta Metall. Sin.(Engl. Lett.)*. 2008;21(1):21-29.
- 5 Sun, Y., Bell, T., Wood, G. Wear behaviour of plasma-nitrided martensitic stainless. *Wear*. 2004;178:131-138.
- 6 Sobieckia JR, Pawel M, Patejuk A. Improving the performance properties of valve martensitic steel by glowdischarge-assisted nitriding. *Vacuum*. 2004;76:57-61.
- 7 Li CX, Bell T. A comparative study of low temperature plasma nitriding, carburising and nitrocarburising of AISI 410 martensitic stainless steel. *Materials Science and Technology*. 2007;23(3):355-361.
- 8 Scheuer CJ, Cardoso RP, Pereira R, Mafra M, Brunatto SF. Low temperature plasma carburizing of martensitic stainless steel. *Materials Science and Engineering A*. 2012;539:369-372.
- 9 Scheuer CJ, Cardoso RP, Zanetti FI, Amaral T, Brunatto SF. Low-temperature plasma carburizing of AISI 420 martensitic stainless steel: Influence of gas mixture and gas flow rate. *Surface & Coatings Technology*. 2012;206:5085-90.
- 10 Scheuer CJ, Cardoso RP, Mafra M, Brunatto SF. AISI 420 martensitic stainless steel low-temperature plasma assisted carburizing kinetics. *Surface Coating & Technology*. 2013;24:30-37.
- 11 Scheuer CJ, Anjos AD, Cardoso RP, Brunatto SF. Low temperature plasma assisted carburizing of AISI 420 martensitic stainless steel: influence of treatment gas pressure. In: 20<sup>o</sup> Congresso Brasileiro de Engenharia e Ciência dos Materiais (CBECIMAT 2012). 04<sup>th</sup> to 08<sup>th</sup> November, Joinville/SC, Brazil, 2012.
- 12 Scheuer CJ, Anjos AD, Cardoso RP, Brunatto SF. Cementação assistida por plasma a baixa temperatura do aço inoxidável martensítico AISI 420: influência da tensão de pico aplicada. In: VII Congresso Nacional de Engenharia Mecânica (CONEM 2012). 31<sup>th</sup> July to 03<sup>th</sup> August, São Luis/MA, Brazil, 2012.
- 13 Rutherford KL, Hutchings IM. Theory and application of a micro-scale abrasive wear test. *Journal of Testing and Evaluation*. 1997;25(2):250-260.
- 14 Ramalho A. Micro-scale abrasive wear of coated surfaces-prediction models. *Surface and Coatings Technology*. 2005;197:358-366.
- 15 Zum Gahr K-H. *Microstructure and Wear of Materials*. Tribology Series, 10. Amsterdam: Elsevier Science Publishers B.V.; 1987.
- 16 Cozza RC, Tanaka DK, Souza RM. Friction coefficient and abrasive wear modes in ball-cratering tests conducted at constant normal force and constant pressure-Preliminary results. *Wear*. 2009;267:61-70.
- 17 Cozza RC, Tanaka DK, Souza RM. Friction coefficient and wear mode transition in micro-scale abrasion tests. *Tribology International*. 2011;44:1878-89.
- 18 Cozza RC. A study on friction coefficient and wear coefficient of coated systems submitted to micro-scale abrasion tests. *Surface and Coatings Technology*. 2013;215:224-233.
- 19 Cozza RC. Influence of the normal force, abrasive slurry concentration and abrasive wear modes on the coefficient of friction in ball-cratering wear tests. *Tribology International*. 2014;70:52-62.
- 20 Cozza RC, Mello JDB, Tanaka DK, Souza RM. Relationship between test severity and wear mode transition in micro-abrasive wear tests. *Wear*. 2007;263:111-116.
- 21 Sevim I, Kulekci MK. Abrasive wear behaviour of bio-active glass ceramics containing apatite. *Bulletin of Material Science*. 2006;29(3):243-249.

\* *Technical contribution to the 1<sup>st</sup> Workshop on surface treatments of corrosion resistant alloys, July 21<sup>st</sup> -25<sup>th</sup>, 2014, São Paulo, SP, Brazil.*